catalysts

MDPI

Article

The Application of Copper-Gold Catalysts in the Selective Oxidation of Glycerol at Acid and Basic Conditions

Piotr Kaminski

Department of Rare Earths, Faculty of Chemistry, Adam Mickiewicz University, ul. Uniwersytetu Poznańskiego 8, 61-614 Poznań, Poland; piotr.kaminski@amu.edu.pl; Tel.: +48-61-829-1832

Abstract: The crude glycerol is produced during the transesterification of animal fats and vegetable oils, but it is a by-product of this process. Currently, its elimination is a problem in the chemical industry. The main goal of this work was the preparation, characterization and application of mesoporous cerium-zirconium oxide as supports for copper and gold species and the comparison of selected factors on the properties of catalysts in glycerol oxidation in the liquid phase. The samples were characterized using adsorption and desorption of nitrogen, XRD, UV-vis, XPS, TEM, SEM, and STEM-EDXS. The obtained results of glycerol oxidation show that the bimetallic copper-gold catalysts are more active and selective to glyceric acid in this reaction than analogous monometallic gold catalysts. Additionally, bimetallic catalysts are also characterized by the catalytic stability, and their application leads to the increase of selectivity to glyceric acid during their reusing in glycerol oxidation in alkali media. In this work, the influence of selected factors, e.g., oxygen source and its pressure, solution pH, and base content on the catalytic activity of bimetallic catalysts is discussed.

Keywords: bimetallic catalysts; mesoporous materials; gold; copper; glycerol oxidation; materials characterisation

Citation: Kaminski, P. The Application of Copper-Gold Catalysts in the Selective Oxidation of Glycerol at Acid and Basic Conditions. *Catalysts* **2021**, *11*, 94. https://doi.org/10.3390/catal11010094

Received: 15 November 2020
Accepted: 10 January 2021
Published: 12 January 2021

1. Introduction

Glycerol is a chemical compound obtained during the transesterification of oils and fats [1,2]. The increase of biodiesel production leads to the surplus of crude glycerol, which cannot be assimilated into traditional glycerol outlets. Glycerol is a highly functionalized reagent that can be applied in the synthesis of fine chemicals such as fuel sources, pharmaceuticals, biodegradable polymers, etc. [3–5]. Various catalytic processes can be used to obtain the valuable chemicals: oxidation, hydrogenolysis, dehydration, etherification, transesterification, etc. [6]. The studies of the catalytic selective oxidation of glycerol over supported Au containing catalysts started in the 1990s [7].

The catalytic oxidation of glycerol is a reaction that can run through multiple pathways and gives various valuable chemicals [8]. The products of glycerol oxidation are, e.g., glyceric acid, tartronic acid, 1,3-dihydroxyacetone and glyceraldehyde [9–12]. The challenge of the petrochemical industry is the development of catalysts for glycerol oxidation, which will be characterized by high activity, selectivity to selected products and catalytic stability.

The proposal mechanisms of glycerol oxidation were reported in References [13,14] and these mechanisms were based on the transformation of glycerol to glyceric (GLA) and tartronic acid (TA), without C-C cleavage, which was explained by the formation of H_2O_2 during the reaction. At the beginning, glycerol molecules are oxidized to glyceraldehyde. In the presence of alkali media, this substrate is rapidly consumed and is transformed to glyceric acid. It was shown that the catalysts modified with noble metals during glycerol oxidation in the basic aqua solution [15–18], can lead to the formation of the products presented in Scheme 1.

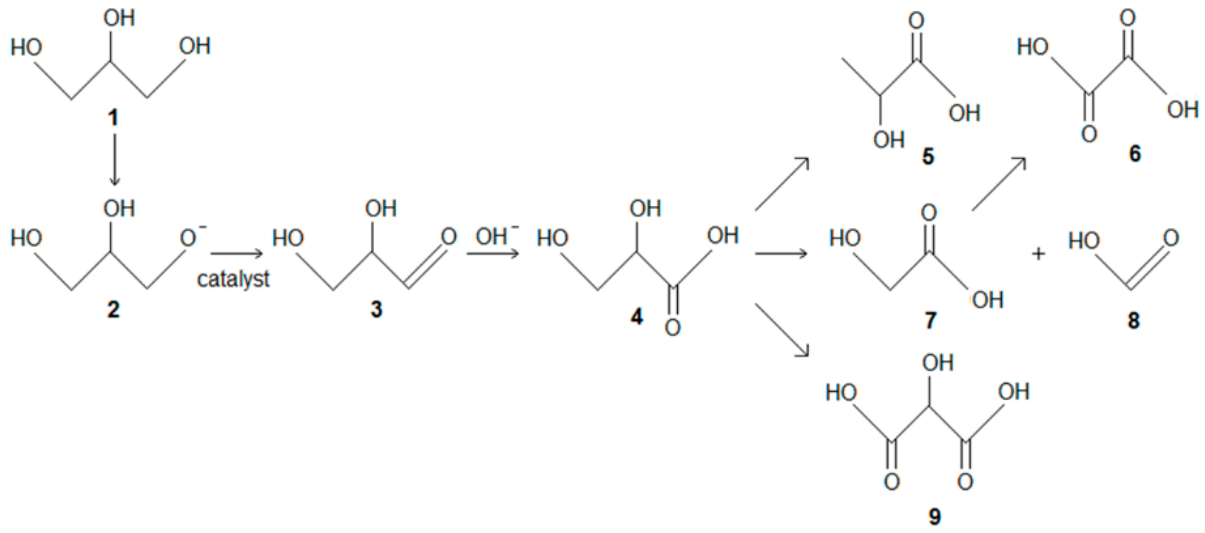

Scheme 1. The products of glycerol oxidation, where (1) glycerol, (2) glycerolate, (3) glyceraldehyde, (4) glyceric acid, (5) lactic acid, (6) oxalic acid, (7) glycolic acid, (8) formic acid, and (9) tartronic acid.

It was described in Reference [12] that the composition of reaction mixture can influence the catalytic properties of catalysts. It was shown that the reaction selectivity over gold catalysts can be controlled by the particle size of noble metal [19] and the properties of the support [20]. It was shown in Reference [21] that the size of gold nanoparticles and their content can lead to high activity in glycerol oxidation. The authors of this research explained this phenomenon that low Au loadings favor the formation of smaller homogenous gold nanoparticles, because these particles are stronger adsorption sites for glycerol molecules. It was also reported that other catalysts, based on noble metals, can be effective for the oxidation of glycerol to glycolic acid in the liquid phase, e.g., about 85% glycerol conversion and 57% selectivity to glycolic acid were obtained over the Ag/Al_2O_3 catalyst [22].

The catalysts modified with copper species in the form of CuO supported on selected oxides such as SiO_2, Al_2O_3, CaO, SrO or ZrO_2 were studied for the synthesis of lactic acid from glycerol in the liquid phase without using reducing or oxidizing agents [23–25]. The studied catalysts achieved high glycerol conversion and the selectivity to lactic acid—the highest selectivity to this acid was obtained over CuO/ZrO_2 catalyst (94.6% yield). It is worth noting that lactic acid and its derivatives are used in the synthesis of biodegradable fibers and other biobased chemicals [23,26].

The catalytic glycerol oxidation has been studied in the aqueous solution at acidic or basic conditions, over the monometallic catalysts, e.g., modified with Au, Pd or Pt or the bimetallic, e.g., Pt-Au or Pd-Au catalysts [27–29]. Regardless of the supporting material, size and morphology of catalytic, metallic gold species, the oxidation of glycerol usually produces fairly high selectivity toward the formation of glyceric acid, and also in smaller concentrations of other acids: glycolic acid, oxalic acid, tartronic acid, lactic acid, etc. [23,25,26,30–33].

Glyceric acid and its derivatives are promising fine chemicals for pharmaceutical or biochemical industry because there are applied, e.g., in the production of medicaments for ethanol and acetaldehyde oxidation [34]. Glyceric acid and its derivatives can also be used in the synthesis of biodegradable surfactants, novel functionalized phospholipid derivatives and phosphatidylcholine analogues [35].

It has been reported in References [13,36–40] that mono, bi and tri-metallic supported catalysts modified with gold species can be applied as the catalysts in this reaction. It was evidenced in References [41,42] that the catalytic efficiency of catalysts in glycerol oxidation can be improved for glycerol oxidation after the addition of monometallic catalyst, the second noble metal such as Au, Pd or Pt. It has been described in Reference [42] that the

introduction of Cu and Ag species on the surface of Au/ZnO catalyst can generate strong metal–metal interactions. It was reported in Reference [43] that the introduction of the second metal to the active phase of catalysts can induce the structural modifications of gold particles. The modification of gold catalysts by the addition of the second metal can improve the selectivity to valuable chemical compounds in oxidation processes because the second metal can play the role of a promoter and it stabilizes the metallic gold particles before their agglomeration. It was presented in Reference [44] that the oxygen adsorption capacity of lactic acid containing perovskite supports for AuPt nanoparticles had a significant influence on the reaction selectivity. An according to the literature data, Au-Pd [45–51], Au-Pt [46,49] and Au-Cu [52–54] catalysts were characterized by a positive interaction between two metals, which can lead to the growth of activity in oxidation processes and the catalytic stability of catalysts.

The catalytic activity of catalysts can be controlled by selected factors of reaction conditions, e.g., solution pH, pressure [55–58] and the physicochemical properties of the catalyst can have a significant effect on the selectivity of each reaction pathway [20].

The main aim of this study is to show that mesoporous cerium-zirconium oxides, and their modification with copper species, can lead to obtaining the active catalysts in selective glycerol oxidation to fine chemicals. The novelty of this work is shown that the factors such as: pH solution, oxygen source and its pressure had an influence on the activity of mesoporous cerium-zirconium oxides modified with copper and gold species in glycerol oxidation. Additionally, the catalytic activity in glycerol oxidation and the selectivity to selected products achieved over the bimetallic copper-gold catalysts were compared to the results obtained over monometallic gold catalysts. The catalysts were deeply characterized before and after their performance in the oxidation process using selected analytical techniques: XRD, XPS, UV-vis spectroscopy and STEM-EDXS.

2. Results and Discussion

2.1. General Characterisation

Selected analytical techniques, e.g., XRD, adsorption and desorption of nitrogen at 77 K, UV-vis, XPS, TEM, SEM, and STEM-EDXS, were applied to the characterization of the structure and texture properties of materials, before and after their performance as catalysts in selective glycerol oxidation. These studies were also performed to obtain information about the chemical composition of catalysts after their reusing in the oxidation process and to estimate the oxidation state of metal species before the application of catalysts in the glycerol oxidation. The comparison of catalysts is described in the paragraph titled "the changes in materials after reaction" (which is the point of Section 2.3 in this work), but the general information about the properties of calcined materials before their application in the catalytic tests are described in this paragraph.

XRD patterns were carried out to obtain information about the crystallinity of oxides, the coordination of selected oxides and the size of metallic gold particles. XRD patterns performed for materials confirmed that all oxides were characterized by crystal phase (Figure 1). Ceria was characterized by the crystal cubic phase. In the case of catalysts with pure zirconia as the support, XRD patterns were characterized of two phases: the tetragonal and monoclinic phase. The XRD patterns of $CeZrO_x$ confirmed the domination of reflections due to the crystal structure of zirconia. It can suggest that, in mixed cerium-zirconium oxide, ceria crystals were located in the structure of zirconia particles. The XRD patterns recorded for bimetallic catalysts showed that the addition of copper species leads to the creation of the crystal phase of metallic gold particles, which has a size bigger than 5 nm (the reflections at 2θ = ~38.2°).

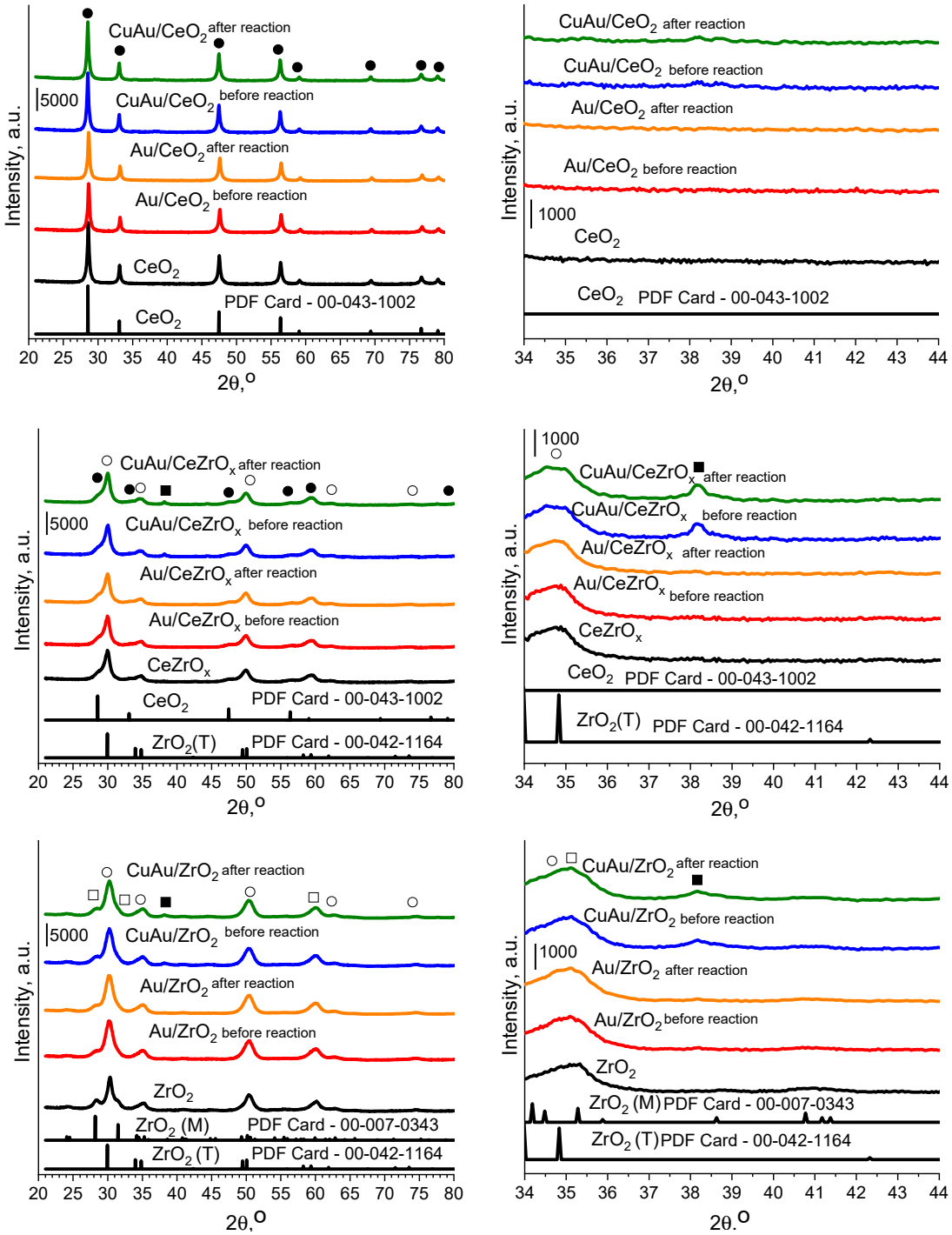

Figure 1. X-ray diffraction (XRD) patterns recorded for materials based on CeO_2, $CeZrO_x$ and ZrO_2 before and after their application as catalysts in glycerol oxidation in alkali media. The reflections were marked using symbols: ● means the crystal phase of ceria in cubic coordination, ○ and □ are due to the crystal phases of zirconia in tetrahedral (T) and monoclinic (M) coordination, respectively, ■ is due to the crystal phase of metallic gold particles.

The nitrogen adsorption and desorption isotherms were applied to estimate the texture parameters of materials (Figure S1). The specific surface area of the catalysts depended on the nature of the supports, and the increase of zirconium content in the oxide distribution led to the growth of this parameter in the following order: CeO_2 (24 m^2 g^{-1}) < $CeZrO_x$ (103 m^2 g^{-1}) < ZrO_2 (121 m^2 g^{-1}). The modification of catalysts with gold and copper species slightly changed the surface area of monometallic oxide supports, whereas the

catalysts based on $CeZrO_x$ revealed much lower surface areas (about 65 m^2 g^{-1}) after their modification with copper and gold species. It can confirm the incorporation of gold and copper species to pores of $CeZrO_x$. More details about the results of the texture parameters of catalysts before their use in glycerol oxidation were reported in Reference [56] and they are shown in this work to outline the general information about the morphology of materials.

TEM images (Figure S2) were recorded for selected materials before their use in glycerol oxidation. These images confirmed the presence of mesopores in the bimetallic catalysts and monometallic gold and/or bimetallic copper-gold particles on the surface of oxides. The TEM images proved that the addition of copper species leads to the decrease of the size of metallic gold particles and/or bimetallic copper-gold particles. The obtained gold or copper-gold particles were between 1.6 nm in $CuAu/ZrO_2$ and 3.6 nm in $CuAu/CeO_2$. The full information about the particle size distribution of gold and copper-gold particles on the surface of oxides was presented in Reference [56] and it was described in this paragraph to outline the general information about this parameter in the studied oxides.

2.2. The Influence of Selected Conditions on the Catalytic Activity and Selectivity

It was reported in References [57,58] that high conversion during the oxidation in the gas phase of different chemical compounds (e.g., methanol or carbon dioxide) can be achieved over the bimetallic copper-gold catalysts. The novelty in this work is the presentation of the influence of selected factors (e.g., oxygen source and its pressure, pH solution, etc.) on the conversion of glycerol in its oxidation in the liquid phase and the selectivity of products over catalysts based on ceria, zirconia, cerium-zirconium oxides modified with gold and copper species.

2.2.1. The Influence of Oxygen Source and pH Solution

The comparison of results in Figures 2 and 3 shows that bimetallic Cu-Au catalysts can achieve high glycerol conversion (>70%) in its oxidation and high selectivity to glyceric acid (65–79%) if the source of oxygen is pure oxygen and the reaction runs in an alkali media. In these conditions, other products created in the liquid phase, e.g., glycolic acid or formic acid, but the selectivity of these compounds were much lower. The results confirm the possibility of creating these products in glycerol oxidation in the presence of alkali media and pure oxygen [13,59–62].

The comparison of the results of glycerol oxidation over copper-gold catalysts in the alkali media using gas oxygen or hydrogen peroxide (Figure 2) as the oxygen source shows that the source of oxygen has a strong influence on the catalytic activity of catalysts. The differences in the mechanism of hydrogen peroxide decomposition can explain this phenomenon. Hydrogen peroxide is unstable in aqua solution which pH is around 13 and it decomposed to water and molecular oxygen [$2\ H_2O_2 \rightarrow 2\ H_2O + O_2$] [63]. The oxygen molecule is created in situ during the reaction of glycerol oxidation and can be a friendly oxidant for the environment. The process of hydrogen peroxide decomposition is more effective at basic conditions than in acid aqua solution, which has a pH around 1. The partial reaction of hydrogen peroxide with nitric acid can explain this process. This reaction leads to the creation of peroxynitric acid [$H_2O_2 + HNO_3 \rightarrow H_2O + HNO_4$] [64]. At basic conditions, the reaction between hydrogen peroxide and sodium hydroxide leads to the attack of anions such as OH^- and HO_2^- and H_2O_2 decomposition. $HO_2^{-\bullet}$ is a vital reactive intermediate, which is created mainly during the reaction between H_2O_2 and NaOH [65].

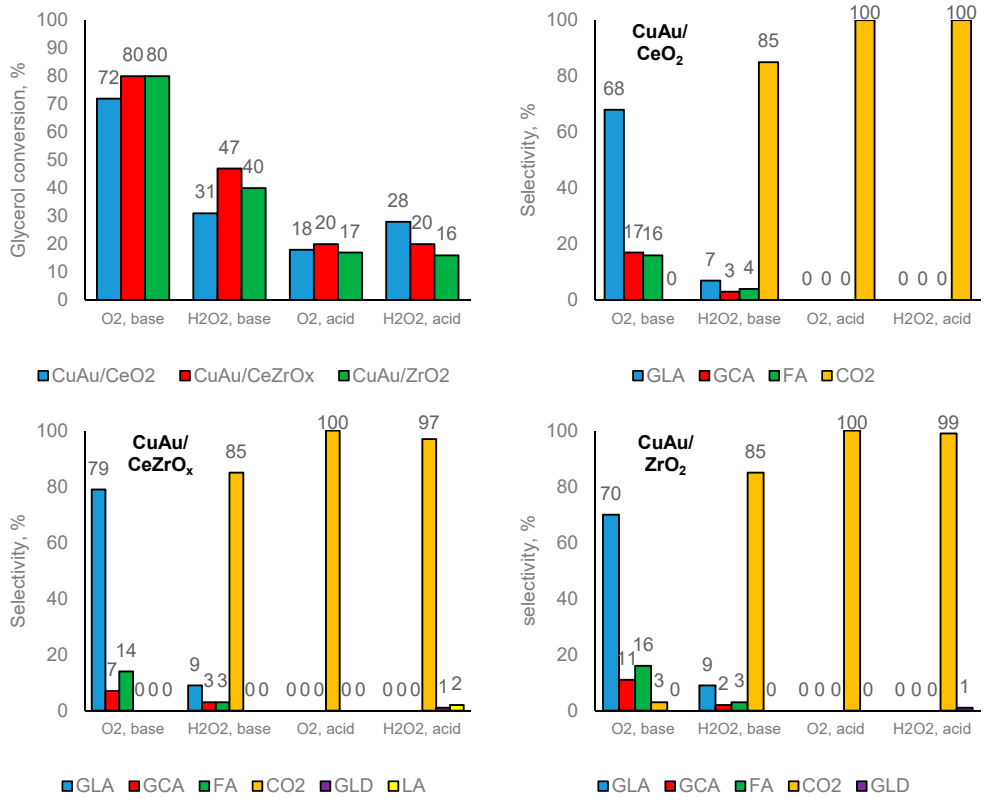

Figure 2. Conversions and selectivities achieved over selected bimetallic copper-gold catalysts in glycerol oxidation in the presence of pure oxygen (6 bars = 5.4 mmol) or hydrogen peroxide (6.6 mmol) and acid (HNO_3) or base (NaOH) in the reaction solution. Reaction conditions: 15.00 g of H_2O; molar ratio NaOH:glycerol = 2:1 (3.0 mmol of NaOH; 1.5 mmol of glycerol) or HNO_3:glycerol = 2:1 (3.0 mmol of HNO_3; 1.5 mmol of glycerol), 30.0 mg catalyst (1.52×10^{-6} mol Au and 8.03×10^{-6} mol Cu in $CuAu/CeO_2$ and $CuAu/CeZrO_x$; 9.14×10^{-7} mol Au and 8.03×10^{-6} mol Cu in $CuAu/ZrO_2$); reaction temperature: 333 K, time: 5 h, stirring speed: 1000 rpm. GLA means glyceric acid, GCA—glycolic acid, FA—formic acid, TA—tartronic acid, GLD—glyceraldehyde, and LA—lactic acid.

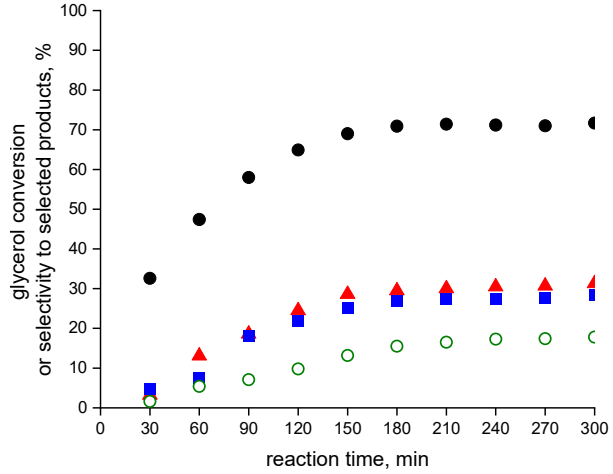

Figure 3. The comparison of glycerol conversions achieved over $CuAu/CeO_2$ catalyst during glycerol oxidation in the presence of oxygen (5.4 mmol) or hydrogen peroxide (6.6 mmol) and base (NaOH) or acid (HNO_3) in the reaction solution, where glycerol conversion over the catalyst in the presence: ●—NaOH and pure oxygen;▲—NaOH and hydrogen peroxide; ■—HNO_3 and hydrogen peroxide; ○—HNO_3 and pure oxygen.

The conversion of glycerol (in the range of 31–47%) in its oxidation over copper-gold catalysts using hydrogen peroxide as the source of oxygen was lower than when pure oxygen was applied and the main product of this process was carbon dioxide. The highest glycerol conversion in its oxidation by hydrogen peroxide was achieved over $CuAu/CeZrO_x$. It can evidence the presence of a positive interaction between cerium and zirconium species based on the electron transfer from oxygen in the crystal structure of oxides and/or hydrogen peroxide molecule to the cations of cerium (Ce^{3+} and Ce^{4+}) and/or zirconium Zr^{4+}. The UV-vis and XPS study proved the presence of these cerium and zirconium species. The obtained results suggest that, in the selective oxidation of glycerol to glyceric acid, the transport of oxygen and its form in aqua solution has an influence on the rate and pathway of glycerol transformation. At acid conditions, glycerol conversion in its oxidation over copper-gold catalysts by hydrogen peroxide was lower (in the range of 16%–28%) than in the alkali media. It is worth noting that, in the case of $CuAu/CeO_2$, higher glycerol conversion in its oxidation at acid conditions was achieved in the presence of H_2O_2 (28%), than in pure oxygen (18%) (Figure 3). This can suggest the positive interaction based on the electron transfer between reduced cerium species (Ce^{3+}) and oxido nitrate anions (NO_4^-). The presence of reduced cerium species (Ce^{3+}) on the external surface of $CuAu/CeO_2$ catalyst after its application in glycerol oxidation using hydrogen peroxide was confirmed using XPS analysis (Figure S3). The distribution of Ce^{3+} species before and after oxidation process was 23% and 25%, respectively. The $CuAu/CeO_2$ catalyst was studied in glycerol oxidation at 333 K for 5 h at 1000 rpm in the presence of other acids—hydrochloric acid (HCl) in the presence of hydrogen peroxide as a source of oxygen. The change of acid did not have an influence on the glycerol conversion and the selectivity of the products of oxidation, because the conversion was 24% and the main product of this reaction was carbon dioxide (99% of selectivity and traces to glyceraldehyde and lactic acid). The achieved results show that chloride ions (Cl^-) can take part in electron transfer during glycerol oxidation and they can generate the $AuCl^-$ species, which can play a role in basic centers [66].

Hydrogen peroxide is known as a strong oxidant applied in the oxidation of chemical compounds in the liquid-phase under very mild reaction conditions. The interaction between hydrogen peroxide and the bimetallic copper-gold active phase of catalysts lead to the creation of gaseous compounds (carbon dioxide and water) during glycerol oxidation. Depending on the properties of the catalyst surface, the different types of O-O bond cleavage in H_2O_2 could occur (homolytic or heterolytic), which generate selected oxidative species. The results of glycerol oxidation to glyceric acid suggest that it was a process run on the catalyst surface, but the formation of this acid was possible mainly in the presence of a base (NaOH) and pure oxygen (O_2) molecules. The glycerol conversion in its oxidation by H_2O_2 was lower, and additionally, glycerol was oxidized to carbon dioxide. It can suggest that the direct introduction of hydrogen peroxide to the basic reaction mixture leads at the beginning to the reaction between H_2O_2 molecules and OH^- ions and the total oxidation of glycerol molecules to carbon dioxide and water.

The results of glycerol oxidation in the presence of hydrogen peroxide and in basic conditions show that the main product of this reaction was carbon dioxide at the selectivity to this product increased from 69% after 30 min to 85% after 300 min, but the highest growth of selectivity is observed in the first two hours (Figure 4). The decrease the selectivity to glyceric and glycolic acid and the slight increase of selectivity to formic acid was also observed. Formic acid and glycolic acid are the products of glyceric acid oxidation and these acids are probably strongly adsorbed on the surface of catalysts and they are oxidized to carbon dioxide.

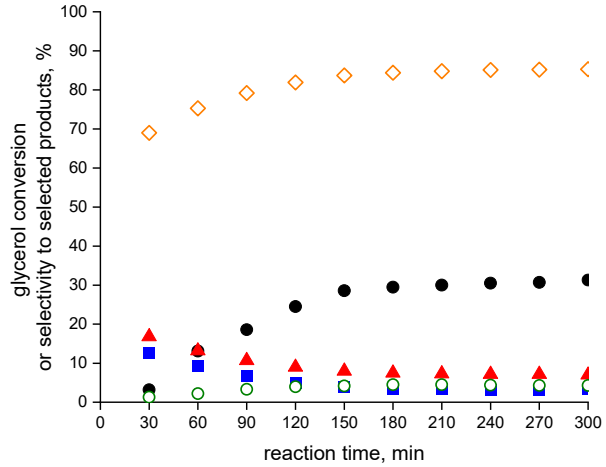

Figure 4. Glycerol conversion and selectivities to selected products achieved over $CuAu/CeO_2$ catalyst during glycerol oxidation in the presence of hydrogen peroxide (6.6 mmol), and base (NaOH) in the reaction solution. Reaction conditions: 15.00 cm^3 of aqua solution; molar ratio NaOH:glycerol = 2:1 (3.0 mmol of NaOH; 1.5 mmol of glycerol), 30.0 mg catalyst (1.52×10^{-6} mol Au and 8.03×10^{-6} mol Cu); reaction temperature: 333 K, time: 5 h, stirring speed: 1000 rpm, where: ●—glycerol conversion; ▲—selectivity to glyceric acid; ■—selectivity to glycolic acid; ○—selectivity to formic acid; ◊—selectivity to carbon dioxide.

2.2.2. The Influence of Catalyst Amount

The influence of different amounts of catalysts on the catalytic activity over copper-gold catalysts was also studied in glycerol oxidation at 333 K for 5 h in alkali media. The results, collected in Table 1, show that the twice smaller amount of catalyst (15 mg) did not lead to the significant drop of glycerol conversion, irrespective of the chemical composition of support, but the smallest decrease (from 80% to 66%) is observed in the case of $CuAu/CeZrO_x$. It can suggest that the presence of the interaction based on the electron transfer between cationic cerium (Ce^{3+}/Ce^{4+}), zirconium (Zr^{4+}) species and metallic species such as metallic gold (Au^0) and copper oxides (mainly CuO) can improve the oxygen transfer on the surface of the catalyst to the active centers. In the case of $CuAu/CeO_2$, the smaller amount of catalyst can lead the growth of selectivity to the product of the total oxidation of glycerol—carbon dioxide. The most interesting results were achieved for $CuAu/ZrO_2$ catalyst, because the selectivity to formic acid at the lower amount of catalyst was 23%, and it can be explained by the presence of small gold particles (the average size of gold particles in $CuAu/ZrO_2$ catalyst was 1.6 nm) and the influence of porosity on the diffusion of reagents. This catalyst was characterized by the high specific surface area (110 m^2/g) (Figure S1). These parameters could have an influence on the slower diffusion glyceric acid and the increase of selectivity of its oxidation at the beginning to glyceric acid, which was oxidized to formic acid.

Table 1. The influence of catalyst amount on the catalytic activity in glycerol oxidation [1].

Catalyst	Conv., %		Selectivity, %									
			GLA [2]		GCA [2]		FA [2]		TA [2]		CO_2	
	15 mg	30 mg	15 mg	30 mg	15 mg	30 mg	15 mg	30 mg	15 mg	30 mg	15 mg	30 mg
$CuAu/CeO_2$	53	72	57	68	9	17	12	16	3	-	19	-
$CuAu/CeZrO_x$	66	80	79	79	7	7	11	14	2	-	1	-
$CuAu/ZrO_2$	64	80	68	70	7	11	23	16	2	-	-	3

[1] Reaction conditions: 15.00 g distilled water, NaOH:glycerol = 2:1, 3.0 mmol NaOH, 1.5 mmol glycerol, 15 or 30 mg od catalyst; 5 h at 333 K at 1200 rpm, p_{O2} = 6 bars; [2] GLA—glyceric acid, GCA—glycolic acid, FA—formic acid, TA—tartronic acid.

2.2.3. The Effect of Oxygen Pressure

The influence of different oxygen pressures on the catalytic activity over copper-gold catalysts was also studied in glycerol oxidation at 333 K for 5 h in alkali media. The results, collected in Figure 5, show that the decreasing of oxygen concentration used to glycerol oxidation from 6 to 3 bars leads to the decrease of conversion. At lower oxygen pressure (3 bars), the selectivity to glyceric acid for all copper-gold catalysts and glycolic acid, excluding $CuAu/CeZrO_x$, decreases and the selectivity to carbon dioxide increases. At lower oxygen contents, cerium-zirconium oxide positively effects glycerol conversion and it can suggest the presence of the interaction between cerium and zirconium species, which improves the catalytic properties of the active phase (the bimetallic Cu-Au system) in the oxidation process. The increase of oxygen content in the autoclave improves not only glycerol conversion in its oxidation, but also the selectivity to glyceric acid, especially over catalysts with cerium species. It suggests that cerium species lead to the increase in the adsorption rate on the surface of catalysts of oxygen molecules and their migration to metallic gold particles. This phenomenon confirms the results presented earlier in References [57,58].

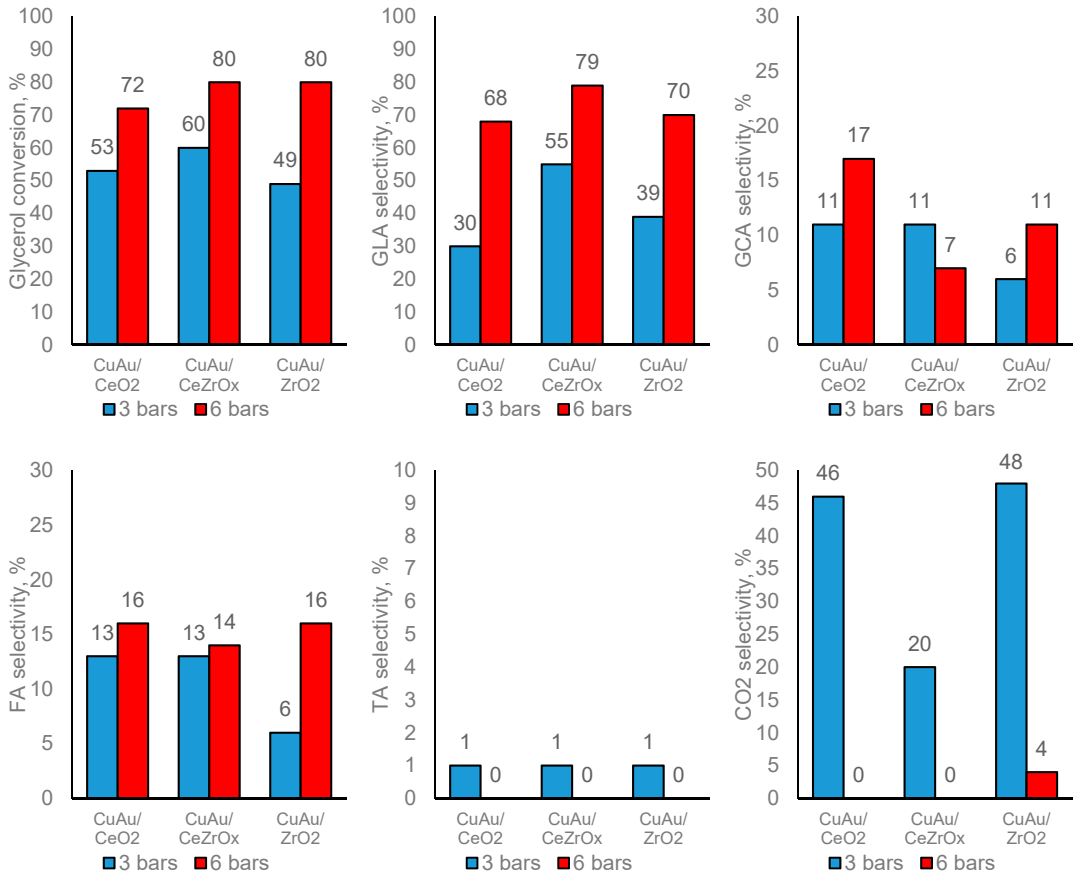

Figure 5. Conversions and selectivities achieved over selected bimetallic copper-gold catalysts in glycerol oxidation in the liquid phase at basic conditions and at different pressure of oxygen at 3 bars (blue column) or 6 bars (red column). Reaction conditions: 15.00 g of H_2O; molar ratio NaOH:glycerol = 2:1 (3.0 mmol of NaOH; 1.5 mmol of glycerol), 30.0 mg catalyst (1.52×10^{-6} mol Au and 8.03×10^{-6} mol Cu in $CuAu/CeO_2$ and $CuAu/CeZrO_x$; 9.14×10^{-7} mol Au and 8.03×10^{-6} mol Cu in $CuAu/ZrO_2$); at 333 K for 5 h. GLA means glyceric acid, GCA—glycolic acid, FA—formic acid, TA—tartronic acid.

The changes during the catalytic process in the molar ratio between oxygen and selected reagents (glycerol, glyceric acid and glycolic acid) were shown in Figure 6 and these correlations were presented for the $CuAu/CeO_2$ catalyst after its application in glycerol oxidation at 333 K for 5 h at 1200 rpm. At the beginning of catalytic oxidation was

observed the highest consumption of glyceric acid and it was represented by the growth of the molar ratio between pure oxygen and glyceric acid. After 180 min of reaction, the content of pure oxygen decreased, because it was consumed in the next steps of oxidation processes, e.g., in the oxidation of glyceric acid to glycolic acid. It is worth noting that, in the case of subsequent reactions, the oxidation of glycerol to glyceric acid and then glyceric acid to glycolic acid, the decrease in the molar ratio between glyceric acid and glycolic acid from 1.90 (after 30 min of reaction) to 1.37 (after 300 min of reaction) was observed, but this ratio decreased to 1.41 after 180 min of reaction. The lack of other products of glycerol oxidation (e.g., formic acid or oxalic acid) can be explained by the strong adsorption of intermediates on the surface of the catalyst and their decomposition to gas products, mainly carbon dioxide.

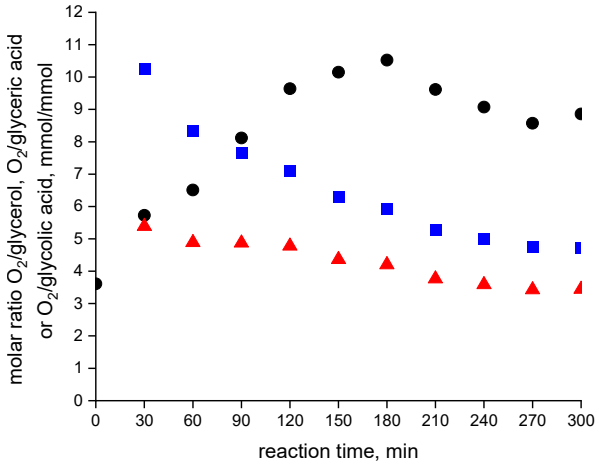

Figure 6. The correlation between molar ratio between O_2 and glycerol, glyceric acid, glycolic acid during the reaction of glycerol oxidation at 333 K for 5 h at 1200 rpm over $CuAu/CeO_2$ catalyst, where: ●—O_2/glycerol; ▲—O_2/glyceric acid and ■—O_2/glycolic acid.

2.2.4. The Influence of Base Content

The correlation between the base concentration in the reaction solution and the catalytic activity was studied for the copper-gold catalysts in glycerol oxidation at 333 K for 5 h in the atmosphere of pure oxygen (6 bars). The results in Figures 2–7 show that a base in aqua solution has a positive effect on glycerol conversion and selectivity to glyceric acid. In the case of $CuAu/ZrO_2$, the conversion of glycerol in its oxidation and the selectivity to glyceric acid did not change when the NaOH content was lower. It means that the first step of this reaction—the dehydrogenation via H-abstraction of one of the primary OH groups of glycerol molecule—does not depend on base concentration in the reaction solution. In the case of $CuAu/CeO_2$, the increase of conversion and the decrease of selectivity are observed when the molar ratio between NaOH and glycerol is 1:1. The growth of selectivity to formic acid or glycolic acid is seen and the decrease of selectivity to glyceric acid at NaOH:glycerol = 1:1 (excluding $CuAu/ZrO_2$). The decrease in the selectivity to glyceric acid and glycolic acid shows that the decrease of base concentration can lead to a change in the pathway of glycerol oxidation.

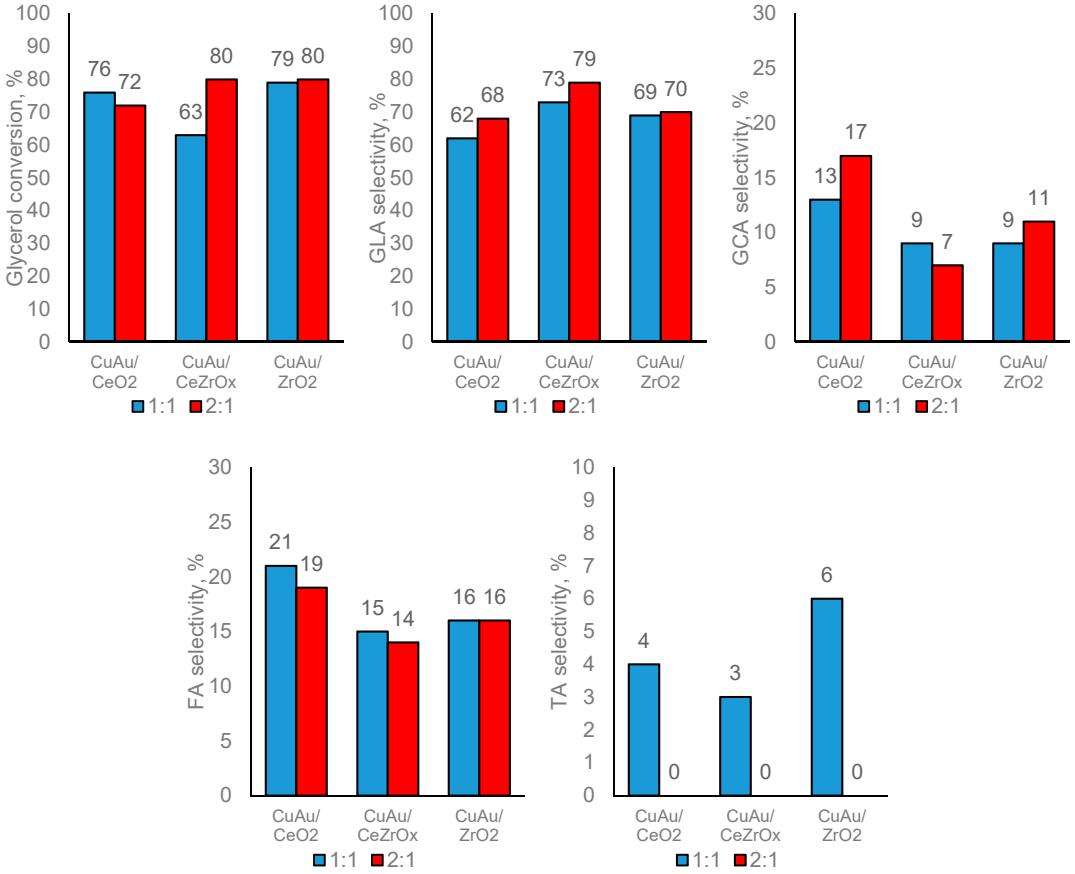

Figure 7. Conversions and selectivities achieved over selected bimetallic copper-gold catalysts in glycerol oxidation in the liquid phase at basic conditions and at different pressure of oxygen (3 or 6 bars). Reaction conditions: 15.00 g of H_2O; molar ratio NaOH:glycerol = 2:1 (3.0 mmol of NaOH; 1.5 mmol of glycerol) or NaOH:glycerol = 1:1 (1.5 mmol of NaOH; 1.5 mmol of glycerol), 30.0 mg catalyst; at 333 K for 5 h. GLA means glyceric acid, GCA—glycolic acid, FA—formic acid, TA—tartronic acid.

2.2.5. The Catalytic Stability

It was published in the literature [36,67] that the catalysts modified with gold species supported on activated carbon or oxides can be applied in glycerol oxidation several times without deactivation. It has been reported in Reference [67] that the best stability in recycling tests in glycerol oxidation was achieved over gold loaded on carbon (better than carbon catalysts modified with palladium or platinum species), showing neither deactivation nor metal leaching. The results of the reusing of gold and copper-gold catalysts in glycerol oxidation are shown in Table 1. It is worth emphasizing that each catalyst used in the first cycle of glycerol oxidation was simply recovered by decantation of the solvent after the reaction and then it was applied in the second cycle without any washing.

The data in Table 2 presents the values of glycerol conversion of achieved over bimetallic catalysts changed after the second cycle of oxidation. After the second cycle, higher selectivity to glyceric acid in glycerol oxidation was obtained over Au/CeO_2 and all bimetallic catalysts. Additionally, on another note, the decreases in the activity can be due to the loss of catalyst during the workup.

Table 2. The reusing of catalysts in glycerol oxidation [1].

Catalyst	Conv., %		Selectivity, %											
			GLA [2]		GCA [2]		FA [2]		TA [2]		LA [2]		CO_2	
	1st	2nd	1st	2nd	1st	2nd	1st	2nd	1st	2nd	1st	2nd	1st	2nd
Au/CeO_2	31	62	18	59	1	3	1	6	-	3	-	-	81	30
$Au/CeZrO_x$	32	25	18	16	1	1	1	1	-	-	-	-	81	82
Au/ZrO_2	19	35	4	3	-	-	-	-	-	-	-	-	96	97
$CuAu/CeO_2$	79	79	54	76	40	8	-	12	-	3	-	-	6	-
$CuAu/CeZrO_x$	85	73	77	81	6	-	8	6	-	2	-	12	10	-
$CuAu/ZrO_2$	83	62	63	93	16	-	4	5	-	2	-	-	17	-

[1] Reaction conditions: 15.00 g distilled water, NaOH:glycerol = 2:1, 3.0 mmol NaOH, 1.5 mmol glycerol, 30 mg od catalyst (1.52×10^{-6} mol Au and 8.03×10^{-6} mol Cu in $CuAu/CeO_2$ and $CuAu/CeZrO_x$; 9.14×10^{-7} mol Au and 8.03×10^{-6} mol Cu in $CuAu/ZrO_2$); 5 h at 333 K at 1200 rpm, p_{O2} = 6 bars; [2] GLA—glyceric acid, GCA—glycolic acid, FA—formic acid, TA—tartronic acid, LA—lactic acid.

2.3. The Changes in Materials after Glycerol Oxidation

The catalysts were studied before and after their application in glycerol oxidation using UV-vis, XRD, TEM and XPS. The aim of these studies was evidenced by the changes in the structure of the catalyst surface after glycerol molecules adsorption and their transformation during oxidation in the liquid phase.

2.3.1. UV-Vis Study

UV-vis spectroscopy can be applied to estimate the oxidation state and the coordination of metals. The UV-vis spectra of studied catalysts before and after their application in glycerol oxidation and their reusing in this oxidation process are shown in Figure 8.

In the case of the UV-vis spectra recorded for the catalysts based on ceria, two bands are seen. They are characteristic of the ligand-metal electron charge transfer from oxygen ion (O^{2-}) to cerium cation (Ce^{4+}). The UV-vis band at around 265 nm can be attributed to cerium cation (Ce^{4+}), which is in the tetrahedral coordination, and the band at around 350 nm can be assigned to cerium cation (Ce^{4+}), which has a coordination number higher than four [68,69]. In the case of catalysts based on $CeZrO_x$ support, only one UV-vis band at around 270 nm is visible with a shoulder at around 220 nm. It can mean that the coordination of cerium species on the surface in the ceria-zirconium mixed oxide is different than in the catalysts based on pure ceria.

The range characteristic of the ligand-metal electron charge transfer between oxygen ions and cerium cations is also typical of the electron charge transfer between ligands and gold cations (Au^{3+} and Au^{+}) [70–76], but the examination of this region cannot be useful for characterization of cationic gold species. The bands are in the range of 500–560 nm and can be attributed to the optical absorption of light excited oscillating conductivity electrons of metallic gold particles called surface plasmon resonance [77–81] and around 540–560 nm can also originate from d-d electron transfer in metallic gold [79–81]. In the case of UV-vis spectra recorded for calcined catalysts, before their drying, the band around 530–560 nm was found only in the UV-vis spectra performed for copper-gold catalysts (Figure 8). This weak band can be found also in the UV-vis spectra recorded for gold catalysts after their drying. The bands at around 530–560 nm became well visible also in the spectra of gold catalysts after the first and the second cycle of oxidation. It is worth noting that these bands are more intense after the reusing of catalysts in glycerol oxidation (excluding $CuAu/CeO_2$). It can suggest that the migration of metallic gold species during the oxidation process on the external surface of support in gold catalysts. This phenomenon was confirmed by XPS measurements and it can explain the increase of glycerol conversion in its oxidation, especially over Au/CeO_2 (Table 1). In the case of Cu-Au catalysts, the bands at around 650 nm can be attributed to the ligand-metal electron charge transfer, e.g., in copper oxides nanoclusters [82,83], in $(Cu\text{-}O\text{-}Cu)^{2+}$ clusters [84–86], inter-valence charge

transfer transitions between copper and other metal ions (gold, cerium and/or zirconium) in the bulk solid solution [87].

The obtained results show that the changes in the UV-vis spectra recorded for the catalysts before and after the application of materials in glycerol oxidation can explain the changes in the chemical composition and the coordination of metallic species in the catalysts during the oxidation process.

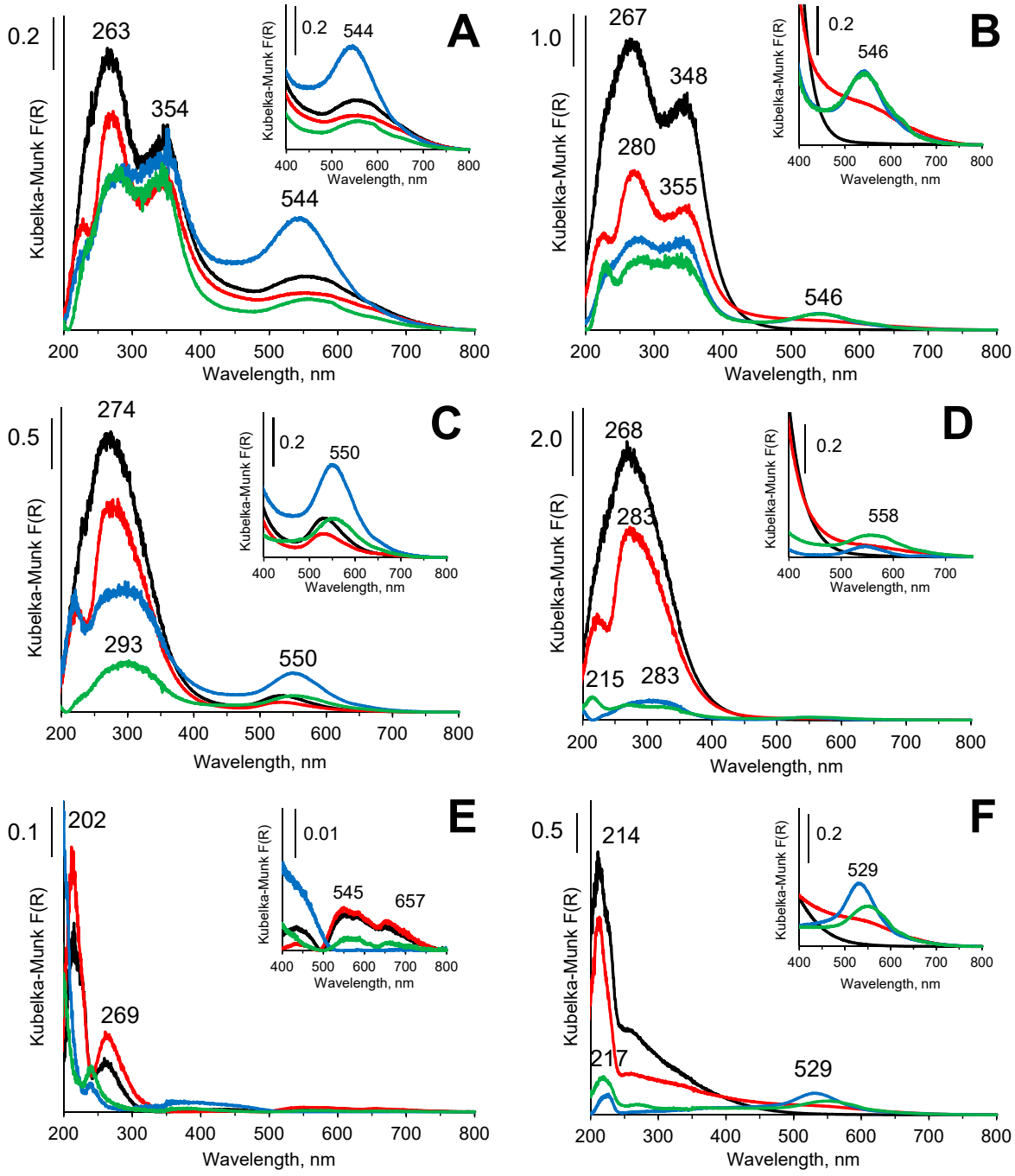

Figure 8. The UV-vis spectra recorded for: (**A**) $CuAu/CeO_2$, (**B**) Au/CeO_2, (**C**) $CuAu/CeZrO_x$, (**D**) $Au/CeZrO_x$, (**E**) $CuAu/ZrO_2$ and (**F**) Au/ZrO_2, before (black line), after drying at 383 K for 13 h (red line), after the first cycle of glycerol oxidation (blue line) and after the second cycle of glycerol oxidation (green line).

2.3.2. XRD Measurements

The XRD patterns were performed for samples before and after their application in glycerol oxidation in alkali media (Figure 1). The comparison of XRD patterns shows that the conditions of reaction slightly changed the crystal phase of materials because the intensity and positions of reflections are similar. It can explain the catalytic stability of catalysts in the second cycle of glycerol oxidation (Table 1).

2.3.3. TEM and STEM-EDXS Analysis

SEM image recorded for $CuAu/ZrO_2$ (Figure S2, left side) confirms the presence of mesopores in the bimetallic catalyst. The TEM image recorded for $CuAu/ZrO_2$ catalyst (Figure S2, right side) confirms the presence of metallic particles (gold and/or copper-gold) whose size is between 2 and 5 nm. It can suggest that the addition of copper species on the surface of gold catalysts leads to the protection of metallic gold particles by their agglomeration. The STEM images (Figure S4) show the presence of bimetallic copper-gold particles in $CuAu/CeZrO_x$, which are smaller than 10 nm, also after glycerol oxidation. It is worth noting that individual bimetallic particles, which increased to around 20 nm after the reaction, are seen. The results obtained using EDX spectroscopy (Figure S4) evidence that the bimetallic copper-gold particles are mainly located on the external surface of materials and the content of gold species in the bulk of materials is much lower than copper species content. It can suggest the migration of copper species during materials modifications with copper and the strong interaction between copper and gold species.

2.3.4. XPS Measurements

The XPS method was applied to estimate the oxidation state of gold, copper and cerium species in the selected catalysts before and after their use in glycerol oxidation and the distribution of these species on the external surface (Figures S5 and S6, Table 3, Tables S1 and S2). The chemical composition of supports has an influence on the changes in the position and intensity of bands in XP spectra.

In the gold catalysts before and after their application in glycerol oxidation, gold species on the external surface were in the metallic (Au^0) and cationic form ($Au^{\delta+}$, where δ means 1 or 3), excluding Au/CeO_2, because in this material, gold was only in the metallic form (Table 3). The changes of gold distribution after glycerol oxidation in all monometallic gold catalysts were slight and the dominant form was metallic gold (Au^0) (Figure S5). Cationic gold species ($Au^{\delta+}$) were formed on cerium-zirconium oxide and pure zirconia in monometallic gold samples and the part of cationic gold species were reduced in these catalysts to metallic form (Au^0) after glycerol oxidation (Table 3). The reduction of a small part of cationic gold ($Au^{\delta+}$) to metallic gold (Au^0) and cationic cerium (from Ce^{4+} to Ce^{3+}) can suggest that the products of glycerol oxidation (CO_2 and/or glyceric acid) had an influence on the partial reduction of gold and cerium species. In the case of bimetallic copper-gold catalysts, the main form of gold was metallic gold (Au^0), but metallic gold species with a partial negative charge on the external surface $(Au^0)^{\delta-}$ appeared and cationic gold ($Au^{\delta+}$) species disappeared in $CuAu/CeO_2$ after glycerol oxidation. However, the distribution of metallic gold species with the partial negative charge on the external surface $(Au^0)^{\delta-}$ decreased after the reaction in the case of bimetallic catalysts with zirconium species. It can suggest that $(Au^0)^{\delta-}$ species are created on the external surface of ceria during glycerol oxidation, especially over the oxidized form of cerium (Ce^{4+}), because the addition of zirconium to the supports led to a bigger growth of reduced form of cerium species (Ce^{3+}) in the distribution of cerium species, especially after the reaction. In the case of $CuAu/CeO_2$, the distribution of cerium species on the external surface before and after the reaction is very similar (23% of cerium is in the reduced form before and 24% after glycerol oxidation).

Table 3. The distribution of gold, copper and cerium species in the studied catalysts, before and after their application in glycerol oxidation.

Catalyst	Distribution of Species (Estimated Using a XPS Method), %							
	Au Species			Cu Species			Ce Species	
	$(Au^0)^{\delta-}$	Au^0	$Au^{\delta+}$	Cu^0	Cu^+	Cu^{2+}	Ce^{3+}	Ce^{4+}
Au/CeO_2 before	-	100	-	-	-	-	29	71
Au/CeO_2 after	-	100	-	-	-	-	34	66
$Au/CeZrO_x$ before	-	84	16	-	-	-	24	76
$Au/CeZrO_x$ after	-	92	8	-	-	-	41	59
Au/ZrO_2 before	-	89	11	-	-	-	-	-
Au/ZrO_2 after	-	93	7	-	-	-	-	-
$CuAu/CeO_2$ before	-	96	4	-	83	17	23	77
$CuAu/CeO_2$ after	18	82	-	10	52	38	24	76
$CuAu/CeZrO_x$ before	19	81	-	-	91	9	18	82
$CuAu/CeZrO_x$ after	8	91	1	16	64	20	39	61
$CuAu/ZrO_2$ before	16	71	13	-	86	14	-	-
$CuAu/ZrO_2$ after	12	88	-	21	33	46	-	-

In all oxides with cerium species, the main form of these species is in the oxidized form (Ce^{4+}) (Table 3), but the presence of zirconium in the mixed oxide has a positive effect on the reduction of cerium species during the reaction of glycerol oxidation. The modification with copper species had an influence on the distribution of the reduced form of cerium species (Ce^{3+}) in bimetallic copper-gold catalysts because it was lower than in the analogues monometallic gold catalysts before their application in glycerol oxidation.

Generally, the presence of cerium and copper species led to the easier reduction of cationic gold in the catalysts before or after their performance in glycerol oxidation than in the case of analogues monometallic gold catalysts. In the monometallic gold and bimetallic copper-gold materials, cationic gold was observed in the case of all catalysts before or after glycerol oxidation (excluding Au/CeO_2), but its distribution was below 20%. The presence of copper species led to the decrease of cationic gold species in gold distribution (excluding $CuAu/CeZrO_x$). Additionally, the growth of copper species on the external surface of catalysts was correlated with the increase of the amount of metallic gold on supports. This can suggest that the co-existence of copper and gold species on the surface of catalysts can be responsible for enhanced core-hole shielding [87].

3. Materials and Methods

3.1. Catalysts Preparation

3.1.1. Preparation of Pure Zirconia, ZrO_2 and Mixed Cerium-Zirconium Oxide, $CeZrO_x$

At the beginning, cetyltrimethylammonium bromide (CTMABr, Sigma-Aldrich, Saint Louis, MO, USA) was dissolved in an aqueous acidic solution (pH = 2 controlled by 35–38% HCl, Chempur, Piekary Śląskie, Poland) at room temperature. Then, the precursors of ceria and zirconia were cerium(III) nitrate ($Ce(NO_3)_3$ 6 H_2O, Sigma-Aldrich) and zirconium *n*-tetrapropanol ($Zr(OC_3H_7)_4$, 70% in 1-propanol, Fluka, Buchs, Switzerland), respectively. These precursors were added to the micellar solution of surfactant and it was assumed the molar ration between the surfactant/precursor of 0.33. After the thermal treatment of this solution at 313 K for 1 h, the synthesis solution was poured into a polypropylene bottle and heated at 353 K for 24 h. The surfactant was removed by ethanol extraction in a Soxhlet apparatus at 351 K for 30 h. The final material was obtained after drying using a vacuum rotator at 343 K and calcination at 673 K for 4 h (the temperature heating rate was 3 K min^{-1}). The nominal (assumed) molar ratio in $CeZrO_x$ between ceria (CeO_2) and zirconia (ZrO_2) was 1:1. It was assumed that 100% of cerium was CeO_2.

3.1.2. Preparation of Pure Ceria, CeO_2

The ethanol solution of Pluronic P-123 (polyethyl glycol-polypropyl glycol–polyethyl glycol, Sigma-Aldrich) was applied to the synthesis of ceria. At the beginning, in 12 cm^3 of ethanol (POCh), the surfactant (1.2 g of Pluronic P-123) and this solution was dissolved and mixed at room temperature for 1 h. Then, the precursor in the form of powder—cerium(III) nitrate ($Ce(NO_3)_3$ 6 H_2O, 99.99%, Sigma-Aldrich) was poured into the surfactant solution. The mixture was stirred for 1 h at room temperature and the final material was obtained after heating the solution to 673 K in air (using a heating rate of 1 K min^{-1}), and at this temperature, the material was calcined for 10 h.

3.1.3. Preparation of Catalysts Modified with Gold Species

At the beginning, 137 mg of tetrachloroauric acid ($HAuCl_4$ 3 H_2O, Johnson-Matthey, London, UK) was dissolved in 217 cm^3 of distillate water. Then, the aqua solution of urea (99%, Fluka, 0.16 mol dm^{-3}) was added to the solution with gold in such a volume to molar ratio between urea and gold was 100. Then, the powder support (4.500 g of selected oxide) was poured into the aqua urea solution with gold. The mixture was stirred at 353 K. After 4 h, the product was filtered and washed using 100 cm^3 of an aqua solution of ammonia (25%, NH_3 H_2O, Chempur) and 850 cm^3 of distilled water to obtain pH = 7. The final materials—Au/CeO_2, $Au/CeZrO_x$, Au/ZrO_2 were dried at room temperature for 24 h under atmospheric pressure and calcined at 623 K for 3 h.

3.1.4. Modification of Gold Catalysts with Copper Species

Copper species were loaded on the surface of gold catalyst by incipient wetness impregnation. At the beginning, the catalyst modified with gold was dried using a vacuum rotator at 348 K. Then, the portion of 2.000 g of dried gold catalyst was impregnated by 2 cm^3 of aqueous solution of $Cu(NO_3)_2$ 2.5 H_2O (0.314 mol dm^{-3}, Sigma-Aldrich). The amount of copper nitrate used for the modification was calculated to achieve the loading of copper equal to 2.0 wt%. The $CuAu/CeO_2$, $CuAu/CeZrO_x$, and $CuAu/ZrO_2$ materials were dried under vacuum at 343 K for 1 h, then at 333 K for 16 h under atmospheric pressure and then calcined at 623 K for 3 h.

3.2. Catalysts Characterisation

In this work, the results of deep characterisation are presented using selected analytical techniques: XRD, adsorption and desorption of nitrogen at 77 K, UV-vis, XPS, TEM, SEM, STEM-EDXS. These techniques were used in the study of catalysts before and after their performance in glycerol oxidation.

3.2.1. X-ray Diffraction (XRD)

XRD measurements (Billerica, MA, USA) were performed using on a Bruker AXS D8 Advance diffractometer equipment with Cu K_α radiation (λ = 0.154 nm), with a step size of 0.05° and in the angle range of 2θ = 21–80°.

3.2.2. The Adsorption and Desorption of Nitrogen

The adsorption and desorption of nitrogen was carried out using a Quantchrome Autosorb iQ Instruments (Odelzhausen, Germany) at 77 K. Before measurements, 0.200 g of powder sample was heated at 573 K for 4 h under high vacuum. The specific surface area was calculated using the Brunauer-Emmett-Teller (BET) method (Odelzhausen, Germany). The Barrett-Joyner-Halenda (BJH) method was applied to estimate the volume of porous and mean pore size.

3.2.3. Ultra-Violet (UV-Vis) Spectroscopy

A Varian-Cary 300 Scan UV-Visible spectrophotometer (Santa Clara, CA, USA) was applied to record the UV-Vis spectra for the catalysts before and after their application in glycerol oxidation and after their drying at RT for 24 h in air atmosphere. In this order, the

samples were placed in a cell equipped with a quartz window. The spectra were recorded in the range of 800–190 nm and Spectralon® was applied as the reference material.

3.2.4. X-ray Photoelectron Spectroscopy (XPS)

X-ray Photoelectron (XP) spectra were recorded using an Ultra High Vacuum (UHV) System (Specs, Berlin, Germany) and the XP spectra were recorded and deconvoluted using OMNIC software (Waltham, MA, USA).

3.2.5. Transmission Electron Microscopy (TEM)

Before measurements using TEM, the powder samples were made in the form of a suspension in 1-butanol and this suspension was deposited on a grid covered with a holey carbon film. The TEM images of samples were carried out using a JEOL 2000 electron microscope operating at 80 kV and the size of the particles was estimated using ImageJ software (Bethesda, MD, USA).

3.2.6. Scanning Transmission Electron Microscopy Combined with Energy Dispersive X-ray Spectroscopy (STEM-EDXS)

The size and form of metallic gold particles were estimated using an aberration-corrected dedicated STEM microscope HD 2700 CS (Hitachi, Chiyoda, Tokyo, Japan) at the operating potential of 200 kV. This microscope was equipment with a high-angle annular dark-field (HAADF) detector (Hitachi, Chiyoda, Tokyo, Japan). The size of the gold particles was estimated using ImageJ software.

3.3. Catalytic Test—Reaction of Glycerol Oxidation

The reaction of glycerol oxidation was carried out in a Berghof-25 (Darmstadt, Germany) autoclave reactor (25 cm^3) using a catalyst suspension in 15.00 g (when the source of oxygen was pure oxygen, O_2, 5.0 N, Linde, Pfungen, Switzerland) or 14.25 g (when the source of oxygen was hydrogen peroxide, H_2O_2, 0.75 g, 30%, Fluka) of distilled water with 1.5 mmol of glycerol (138 mg, >99.0%, Sigma-Aldrich) and 1.5 or 3.0 mmol of NaOH (60 or 120 mg, >99.0%, Merck, Darmstadt, Germany) or 0.028 mmol of HNO_3 (2.7 mg, 65%, Sigma-Aldrich, Saint Louis, MO, USA). The reaction was conducted at 333 K at selected stirring speeds (1000 or 1200 rpm) at 3 or 6 bars of oxygen or in the presence of hydrogen peroxide. The assumed molar ratio between hydrogen peroxide and glycerol was 6.6:1.5 = 4.4. This molar ratio was similar to molar ratio between pure oxygen (6 bars) and glycerol, because in this case, the ratio was 5.4:1.5 = 3.6. The assumed content of hydrogen peroxide was higher, because the part of hydrogen peroxide (around 20%) was decomposed after its addition to the solution, before the addition of catalyst and main oxidation process. The liquid products and un-reacted glycerol were determined quantitatively by a HPLC system equipped with RI and UV-vis detectors.

4. Conclusions

The results of the selective oxidation of glycerol over the mesoporous ceria, zirconia or cerium-zirconium oxide modified with copper and gold species show that the bimetallic copper-gold catalysts can be attractive catalysts for the oxidation of organic compounds in the liquid phase. The most valuable results were achieved over the bimetallic catalysts in glycerol oxidation in the presence of pure oxygen under the pressure of six bars and a molar ratio between NaOH and glycerol was 2:1. The results show the influence of selected factors on the catalytic activity of copper-gold catalysts deposited on ceria, zirconia or cerium-zirconium oxide are collected in Table 4.

Table 4. A table summarizing the different factors on the catalytic activity of copper-gold catalysts.

Catalyst	Effect of Selected Factors on the Glycerol Conversion in Its Oxidation, %							
	pH Solution and Oxygen Source				Oxygen Pressure, Bar		Molar Ratio (NaOH/Glycerol)	
	NaOH and O_2	**NaOH and H_2O_2**	**HNO_3 and O_2**	**HNO_3 and H_2O_2**	**3**	**6**	**1:1**	**2:1**
$CuAu/CeO_2$	72	31	18	28	53	72	76	72
$CuAu/CeZrO_x$	80	47	20	20	60	80	63	80
$CuAu/ZrO_2$	80	40	17	16	49	80	79	80
main product	GLA	CO_2	CO_2	CO_2	GLA/CO_2	GLA	GLA	GLA

GLA—glycolic acid; FA—formic acid; CO_2 – carbon dioxide.

The increase of zirconium content in the support has a positive effect on the catalytic stability and the growth of selectivity to the product of glycerol oxidation—glyceric acid. The highest selectivity to this acid (93%) was achieved in alkali media at 333 K at 1200 rpm over $CuAu/ZrO_2$ after the second cycle of glycerol oxidation. The results of this work show that the bimetallic catalysts can achieve higher activity than analogues gold catalysts not only in the oxidation process in the gas phase [88,89], but also in the liquid phase. Gold catalysts modified with copper species are characterized by the appearance of the electron interaction between both metals. The reduction of copper species was evidenced by the UV-vis and XPS study and the higher mobility of oxygen-promoting oxidative properties was confirmed by XPS measurements. Copper has the larger electron-donating ability and it can modify the electronic properties of metallic gold. The achieved results of glycerol oxidation show that the chemical composition of support, the texture and structure properties of catalysts and the reaction conditions such as the source of oxygen, pH solution, the concentration of OH^- anions, and oxygen content can determine the effectiveness of glycerol oxidation.

Supplementary Materials: The following are available online at https://www.mdpi.com/2073-4344/11/1/94/s1, Figure S1: Isotherms of adsorption and desorption of nitrogen at 77 K performed for: (A) CeO_2; (B) Au/CeO_2; (C) $CuAu/CeO_2$; (D) ZrO_2; (E) Au/ZrO_2 and (F) $CuAu/ZrO_2$, before their application as catalysts in glycerol oxidation, Figure S2: The SEM (left side) and TEM (right side) images recorded for $CuAu/ZrO_2$ before its application in glycerol oxidation, Figure S3: The XP spectra of 3d Ce species region recorded for $CuAu/CeO_2$ after its application as catalyst in glycerol oxidation in the presence of hydrogen peroxide, Figure S4: STEM images and EDX spectra recorded for $CuAu/CeZrO_x$ before and after its application as catalyst in glycerol oxidation, Figure S5: XP spectra of 4f Au species region recorded for: (A) Au/CeO_2; (B) $Au/CeZrO_x$ and (C) Au/ZrO_2 before and after their application as catalysts in glycerol oxidation, Figure S6: XPS spectra of 4f Au species region recorded for: (A) $CuAu/CeO_2$; (B) $CuAu/CeZrO_x$ and (C) $CuAu/ZrO_2$ before and after their application as catalysts in glycerol oxidation, Table S1: The composition of catalysts (estimated using XPS) before and after their application in glycerol oxidation at 333 K for 5 h at 1200 rpm at basic conditions, Table S2: The BE of gold and copper species in the selected catalysts before and after their application in glycerol oxidation.

Funding: This research was funded by the National Science Centre in Cracow in Poland grant number [2015/16/T/ST5/00263] and the Scientific Exchange Programme Sciex-NMSch grant number [12.258]. The APC was funded by MDPI.

Institutional Review Board Statement: Not applicable.

Informed Consent Statement: Not applicable.

Data Availability Statement: The data presented in this study are available on request from the corresponding author. Data is contained within the article or supplementary material.

Acknowledgments: The author would like to acknowledge for the financial support the National Science Centre in Cracow in Poland (project No. 2015/16/T/ST5/00263) and the Scientific Exchange Programme Sciex-NMS^{ch} (application No. 12.258). The author thanks ETH in Zurich (Switzerland) for the STEM-EDXS measurements and sharing the HPLC equipment. P. Kaminski would like to

thank Maria Ziolek (Adam Mickiewicz University in Poznan, the Faculty of Chemistry) and Jeroen A. van Bokhoven (ETH Zurich) for a fruitful discussion and value remarks.

Conflicts of Interest: The author declares no conflict of interest. The founding sponsors had no role in the design of the study; in the collection, analyses, or interpretation of data; in the writing of the manuscript, and in the decision to publish the results.

References

1. Fukuda, H.; Kondo, A.; Noda, H. Biodiesel fuel production by transesterification of oils. *J. Biosci. Bioeng.* **2001**, *92*, 405–416. [CrossRef]
2. Ma, F.; Hanna, M.A. Biodiesel production: A review. *Bioresour. Technol.* **1999**, *70*, 1–15. [CrossRef]
3. Behr, A.; Eilting, J.; Irawadi, K.; Leschinski, J.; Lindner, F. Improved utilisation of renewable resources: New important derivatives of glycerol. *Green Chem.* **2008**, *10*, 13–30. [CrossRef]
4. Pagliaro, M.; Ciriminna, R.; Kimura, H.; Rossi, M.; Pina, C.D. Recent progress on innovative and potential technologies for glycerol transformation into fuel additives: A critical review. *Angew. Chem. Int. Ed.* **2007**, *46*, 4434–4440. [CrossRef]
5. Ten Dam, J.; Hanefeld, U. Renewable chemicals: Dehydroxylation of glycerol and polyols. *ChemSusChem* **2001**, *4*, 1017–1034. [CrossRef]
6. Zheng, Y.; Chen, X.; Shen, Y. Commodity chemicals derived from glycerol, an important biorefinery feedstock. *Chem. Rev.* **2008**, *108*, 5253–5277. [CrossRef]
7. Kimura, H. Selective oxidation of glycerol on a platinum-bismuth catalyst by using a fixed bed reactor. *Appl. Catal. A Gen.* **1993**, *105*, 147–158. [CrossRef]
8. Dodekatos, G.; Tüysüz, H. Effect of Post-Treatment on Structure and Catalytic Activity of CuCo-based Materials for Glycerol Oxidation. *ChemCatChem* **2017**, *9*, 610–619. [CrossRef]
9. Carrettin, S.; McMorn, P.; Johnston, P.; Griffin, K.; Hutchings, G.J. Selective oxidation of glycerol to glyceric acid using a gold catalyst in aqueous sodium hydroxide. *Chem. Commun.* **2002**, 696–697. [CrossRef]
10. Demirel-Gülen, S.; Lucas, M.; Waerna, J.; Salmi, T.; Murzin, D.; Claus, P. Reaction kinetics and modelling of the gold catalysed glycerol oxidation. *Top. Catal.* **2007**, *44*, 299–305. [CrossRef]
11. Ketchie, W.C.; Murayama, M.; Davis, R.J. Promotional effect of hydroxyl on the aqueous phase oxidation of carbon monoxide and glycerol over supported Au catalysts. *Top. Catal.* **2007**, *44*, 307–317. [CrossRef]
12. Zope, B.N.; Hibbitts, D.D.; Neurock, M.; Davis, R.J. Reactivity of the gold/water interface during selective oxidation catalysis. *Science* **2010**, *330*, 74–78. [CrossRef] [PubMed]
13. Ketchie, W.C.; Fang, L.Y.; Wong, M.S.; Murayama, M.; Davis, R.J. Influence of gold particle size on the aqueous-phase oxidation of carbon monoxide and glycerol. *J. Catal.* **2007**, *250*, 94–101. [CrossRef]
14. Villa, A.; Veith, G.M.; Ferri, D.; Weidenkaff, A.; Perry, K.A.; Campisi, S.; Prati, L. NiO as a peculiar support for metal nanoparticles in polyols oxidation. *Catal. Sci. Technol.* **2013**, *3*, 394–399. [CrossRef]
15. Komanoya, T.; Suzuki, A.; Nakajima, K.; Kitano, M.; Kamata, K.; Hara, M. A Combined Catalyst of Pt Nanoparticles and TiO_2 with Water-Tolerant Lewis Acid Sites for One-Pot Conversion of Glycerol to Lactic Acid. *ChemCatChem* **2016**, *8*, 1094–1099. [CrossRef]
16. Redina, E.A.; Kirichenko, O.A.; Greish, A.A.; Kucherov, A.V.; Tkachenko, O.P.; Kapustin, G.I.; Mishin, I.V.; Kustov, L.M. Preparation of bimetallic gold catalysts by redox reaction on oxide-supported metals for green chemistry applications. *Catal. Today* **2015**, *246*, 216–231. [CrossRef]
17. Purushothaman, R.K.P.; van Haveren, J.; van Es, D.S.; Melián-Cabrera, I.; Meeldijk, J.D.; Heeres, H.J. An efficient one pot conversion of glycerol to lactic acid using bimetallic gold-platinum catalysts on a nanocrystalline CeO_2 support. *Appl. Catal. B Environ.* **2014**, *147*, 92–100. [CrossRef]
18. Shen, Y.; Zhang, S.; Li, H.; Ren, Y.; Liu, H. Efficient Synthesis of Lactic Acid by Aerobic Oxidation of Glycerol on Au–Pt/TiO_2 Catalysts. *Chem. Eur. J.* **2010**, *16*, 7368–7371. [CrossRef]
19. Dimitratos, N.; Lopez-Sanchez, J.A.; Lennon, D.; Porta, F.; Prati, L.; Villa, A. Effect of Particle Size on Monometallic and Bimetallic (Au,Pd)/C on the Liquid Phase Oxidation of Glycerol. *Catal. Lett.* **2006**, *108*, 147–153. [CrossRef]
20. Villa, A.; Campisi, S.; Mohammed, K.M.H.; Dimitratos, N.; Vindigni, F.; Manzoli, M.; Jones, W.; Bowker, M.; Hutchings, G.J.; Prati, L. Tailoring the selectivity of glycerol oxidation by tuning the acid–base properties of Au catalysts. *Catal. Sci. Technol.* **2015**, *5*, 1126–1132. [CrossRef]
21. D'Agostino, C.; Brett, G.; Divitini, G.; Ducati, C.; Hutchings, G.J.; Mantle, M.D.; Gladden, L.F. Increased Affinity of Small Gold Particles for Glycerol Oxidation over Au/TiO_2 Probed by NMR Relaxation Methods. *ACS Catal.* **2017**, *7*, 4235–4241. [CrossRef]
22. Díaz, J.A.; Skrzyńska, E.; Zaid, S.; Girardon, J.; Capron, M.; Dumeignil, F.; Fongarland, P. Kinetic modelling of the glycerol oxidation in the liquid phase: Comparison of Pt, Au and Ag AS active phases. *J. Chem. Technol. Biotechnol.* **2017**, *92*, 2267–2275. [CrossRef]
23. Yang, G.-Y.; Ke, Y.-H.; Ren, H.-F.; Liu, C.-L.; Yang, R.-Z.; Dong, W.-S. The conversion of glycerol to lactic acid catalyzed by ZrO_2-supported CuO catalysts. *Chem. Eng. J.* **2016**, *283*, 759–767. [CrossRef]
24. Abdullah, R.; Abdullah, A.Z. Effect of catalyst to glycerol ratio in the production of lactic acid via hydrothermal reaction using calcium oxide and strontium oxide catalysts. *AIP Conf. Proc.* **2018**, *2030*, 020197. [CrossRef]

25. Palacio, R.; Torres, S.; Lopez, D.; Hernandez, D. Selective glycerol conversion to lactic acid on Co_3O_4/CeO_2 catalysts. *Catal. Today* **2018**, *302*, 196–202. [CrossRef]
26. De Clercq, R.; Dusselier, M.; Makshin, E.; Sels, B.F. Catalytic Gas-Phase Production of Lactide from Renewable Alkyl Lactates. *Angew. Chem. Int. Ed.* **2018**, *57*, 3074–3078. [CrossRef]
27. Bianchini, C.; Shen, P.K. Palladium-based electrocatalysts for alcohol oxidation in half cells and in direct alcohol fuel cells. *Chem. Rev.* **2009**, *109*, 4183–4206. [CrossRef]
28. Carrettin, S.; McMorn, P.; Johnston, P.; Griffin, K.; Kiely, C.J.; Hutchings, G.J. Oxidation of glycerol using supported Pt, Pd and Au catalysts. *Phys. Chem. Chem. Phys.* **2003**, *5*, 1329–1336. [CrossRef]
29. Porta, F.; Prati, L. Selective oxidation of glycerol to sodium glycerate with gold-on-carbon catalyst: An insight into reaction selectivity. *J. Catal.* **2004**, *224*, 397–403. [CrossRef]
30. Rodriguez, A.A.; Williams, C.T.; Monnier, J.R. Selective liquid-phase oxidation of glycerol over Au–Pd/C bimetallic catalysts prepared by electroless deposition. *Appl. Catal. A Gen.* **2014**, *475*, 161–168. [CrossRef]
31. Liu, X.; Wang, A.; Wang, X.; Mou, C.Y.; Zhang, T. Au-Cu Alloy nanoparticles confined in SBA-15 as a highly efficient catalyst for CO oxidation. *Chem. Commun.* **2008**, *27*, 3187–3189. [CrossRef] [PubMed]
32. Zavrazhnov, S.A.; Esipovich, A.L.; Zlobin, S.Y.; Belousov, A.S.; Vorotyntsev, A.V. Mechanism Analysis and Kinetic Modelling of Cu NPs Catalysed Glycerol Conversion into Lactic Acid. *Catalysts* **2019**, *9*, 231. [CrossRef]
33. Arcanjo, M.R.A.; da Silva, I.J.; Cavalcante, C.L.; Iglesias, J.; Morales, G.; Paniagua, M.; Melero, J.A.; Vieira, R.S. Glycerol valorization: Conversion to lactic acid by heterogeneous catalysis and separation by ion exchange chromatography. *Biofuels Bioprod. Biorefin.* **2019**, *14*, 357–370. [CrossRef]
34. Eriksson, C.J.P.; Saarenmaa, T.P.S.; Bykov, I.L.; Heino, P.U. Acceleration of ethanol and acetaldehyde oxidation by D-glycerate in rats. *Metabolism* **2007**, *56*, 895–898. [CrossRef]
35. Rosseto, R.; Tcacenco, C.M.; Ranganathan, R.; Hajdu, J. Synthesis of phosphatidylcholine analogues derived from glyceric acid: A new class of biologically active phospholipid compounds. *Tetrahedron Lett.* **2008**, *49*, 3500–3503. [CrossRef]
36. Prati, L.; Rossi, M. Gold on Carbon as a New Catalyst for Selective Liquid Phase Oxidation of Diols. *J. Catal.* **1998**, *176*, 552–560. [CrossRef]
37. Prati, L.; Martra, G. New gold catalysts for liquid phase oxidation. *Gold Bull.* **1999**, *32*, 96–101. [CrossRef]
38. Villa, A.; Wang, D.; Veith, G.M.; Prati, L. Bismuth as a modifier of Au–Pd catalyst: Enhancing selectivity in alcohol oxidation by suppressing parallel reaction. *J. Catal.* **2012**, *292*, 73–80. [CrossRef]
39. Kondrat, S.A.; Miedziak, P.J.; Douthwaite, M.; Brett, G.L.; Davies, T.E.; Morgan, D.J.; Edwards, J.K.; Knight, D.W.; Kiely, C.J.; Taylor, S.H.; et al. Base-Free Oxidation of Glycerol Using Titania-Supported Trimetallic Au–Pd–Pt Nanoparticles. *ChemSusChem* **2014**, *7*, 1326–1334. [CrossRef]
40. Xu, J.; Zhang, H.; Zhao, Y.; Yu, B.; Chen, S.; Li, Y.; Hao, L.; Liu, Z. Selective oxidation of glycerol to lactic acid under acidic conditions using AuPd/TiO_2 catalyst. *Green Chem.* **2013**, *15*, 1520–1525. [CrossRef]
41. Zaid, S.; Skrzyńska, E.; Addad, A.; Nandi, S.; Jalowiecki-Duhamel, L.; Girardon, J.-S.; Capron, M.; Dumeignil, F. Development of silver based catalysts promoted by noble metal M (M = Au, Pd or Pt) for glycerol oxidation in liquid phase. *Top. Catal.* **2017**, *60*, 1072–1081. [CrossRef]
42. Kaskow, I.; Decyk, P.; Sobczak, I. The effect of copper and silver on the properties of Au-ZnO catalyst and its activity in glycerol oxidation. *Appl. Surf. Sci.* **2018**, *444*, 197–207. [CrossRef]
43. Frassoldati, A.; Pinel, C.; Besson, M. Promoting effect of water for aliphatic primary and secondary alcohol oxidation over platinum catalysts in dioxane/aqueous solution media. *Catal. Today* **2013**, *173*, 81–88. [CrossRef]
44. Douthwaite, M.; Powell, N.; Taylor, A.; Ford, G.; López, J.M.; Solsona, B.; Yang, N.; Sanahuja-Parejo, O.; He, Q.; Morgan, D.J.; et al. Glycerol Selective Oxidation to Lactic Acid over AuPt Nanoparticles; Enhancing Reaction Selectivity and Understanding by Support Modification. *ChemCatChem* **2020**, *12*, 1–12. [CrossRef]
45. Mallat, T.; Baiker, A. Oxidation of alcohols with molecular oxygen on platinum metal catalysts in aqueous solutions. *Catal. Today* **1994**, *19*, 247–283. [CrossRef]
46. Gangwal, V.R.; van del Schaaf, J.; Kuster, B.F.M.; Schouten, J.C. Influence of pH on noble metal catalysed alcohol oxidation: Reaction kinetics and modelling. *J. Catal.* **2005**, *229*, 389–403. [CrossRef]
47. Abad, A.; Almela, C.; Corma, C.; Garcia, H. Unique gold chemoselectivity for the aerobic oxidation of allylic alcohols. *Tetrahedron* **2006**, *62*, 6666–6672. [CrossRef]
48. Hou, W.; Dehm, N.A.; Scott, R.W.J. Alcohol oxidations in aqueous solutions using Au, Pd, and bimetallic AuPd nanoparticle catalysts. *J. Catal.* **2008**, *253*, 22–27. [CrossRef]
49. Hutchings, G.J.; Kiely, C.J. Strategies for the synthesis of supported gold palladium nanoparticles with controlled morphology and composition. *Acc. Chem. Res.* **2013**, *46*, 1759–1772. [CrossRef]
50. Marx, S.; Baiker, A. Beneficial Interaction of Gold and Palladium in Bimetallic Catalysts for the Selective Oxidation of Benzyl Alcohol. *J. Phys. Chem. C* **2009**, *113*, 6191–6201. [CrossRef]
51. Kaizuka, K.; Miyamura, H.; Kobayashi, S. Remarkable effect of bimetallic nanocluster catalysts for aerobic oxidation of alcohols: Combining metals changes the activities and the reaction pathways to aldehydes/carboxylic acids or esters. *J. Am. Chem. Soc.* **2010**, *132*, 15096–15098. [CrossRef] [PubMed]

52. Dimitratos, N.; Villa, A.; Wang, D.; Porta, F.; Su, D.; Prati, L. Pd and Pt catalysts modified by alloying with Au in the selective oxidation of alcohols. *J. Catal.* **2006**, *244*, 113–121. [CrossRef]
53. Prati, L.; Villa, A.; Porta, F.; Wang, D.; Su, D. Single-phase gold/palladium catalyst: The nature of synergetic effect. *Catal. Today* **2007**, *122*, 386–390. [CrossRef]
54. Bauer, J.C.; Veith, G.M.; Allard, L.F.; Oyola, Y.; Overbury, S.H.; Dai, S. Silica-Supported Au–CuO_x Hybrid Nanocrystals as Active and Selective Catalysts for the Formation of Acetaldehyde from the Oxidation of Ethanol. *ACS Catal.* **2012**, *2*, 2537–2546. [CrossRef]
55. Zhao, G.F.; Hu, H.Y.; Deng, M.M.; Ling, M.; Lu, Y. Foam/fiber-structured catalysts: Non-dip-coating fabrication strategy and applications in heterogeneous catalysis. *Green Chem.* **2013**, *13*, 55–58. [CrossRef]
56. Kaminski, P.; Ziolek, M.; van Bokhoven, J.A. Mesoporous cerium–zirconium oxides modified with gold and copper–synthesis, characterization and performance in selective oxidation of glycerol. *RSC Adv.* **2017**, *7*, 7801–7819. [CrossRef]
57. Kaminski, P.; Ziolek, M.; Campo, B.; Daturi, M. FTIR spectroscopic study of CO oxidation on bimetallic catalysts. *Catal. Today* **2015**, *243*, 218–227. [CrossRef]
58. Kaminski, P.; Ziolek, M. Mobility of gold, copper and cerium species in Au, Cu/Ce, Zr-oxides and its impact on total oxidation of methanol. *Appl. Catal. B Environ.* **2016**, *187*, 328–341. [CrossRef]
59. Dimitratos, N.; Villa, A.; Bianchi, C.L.; Prati, L.; Makkee, M. Gold on titania: Effect of preparation method in the liquid phase oxidation. *Appl. Catal. A Gen.* **2006**, *311*, 185–192. [CrossRef]
60. Prati, L.; Spontoni, P.; Gaiassi, A. From renewable to fine chemicals through selective oxidation: The case of glycerol. *Top. Catal.* **2009**, *52*, 288–296. [CrossRef]
61. Veith, G.M.; Lupini, A.R.; Pennycook, S.J.; Villa, A.; Prati, L.; Dudney, N.J. Magnetron sputtering of gold nanoparticles onto WO_3 and activated carbon. *Catal. Today* **2007**, *122*, 248–253. [CrossRef]
62. Villa, A.; Gaiassi, A.; Rossetti, I.; Bianchi, C.L.; Benthem, K.; van Veith, G.M.; Prati, L. Au on $MgAl_2O_4$ spinels: The effect of support surface properties in glycerol oxidation. *J. Catal.* **2010**, *275*, 108–116. [CrossRef]
63. Campos-Martin, J.M.; Blanco-Brieva, G.; Fierro, J.L.G. Hydrogen Peroxide Synthesis: An Outlook beyond the Anthraquinone Process. *Angew. Chem. Int. Ed.* **2006**, *45*, 6962–6984. [CrossRef] [PubMed]
64. Miyamoto, S.; Ronsein, G.E.; Corrêa, T.C.; Martinez, R.G.; Medeiros, M.H.G.; Di Mascio, P. Direct evidence of singlet molecular oxygen generation from peroxynitrate, a decomposition product of peroxynitrite. *Dalton Trans.* **2009**, 5720–5729. [CrossRef] [PubMed]
65. Guo, T.X.; Zhao, Y.; Ma, S.C.; Liu, S.T. Decomposition Characteristics of Hydrogen Peroxide in Sodium Hydroxide Solution. *Adv. Mater. Res.* **2013**, *610–613*, 359–362. [CrossRef]
66. Sobczak, I.; Kusior, A.; Grams, J.; Ziolek, M. The role of chlorine in the generation of catalytic active species located in Au-containing MCM-41 materials. *J. Catal.* **2007**, *245*, 259–266. [CrossRef]
67. Sobczak, I.; Jagodzinska, K.; Ziolek, M. Glycerol oxidation on gold catalysts supported on group five metal oxides–A comparative study with other metal oxides and carbon based catalysts. *Catal. Today* **2010**, *158*, 121–129. [CrossRef]
68. Escamilla-Perea, L.; Nava, R.; Pawelec, B.; Rosmaninho, M.G.; Peza-Ledesma, C.L.; Fierro, J.L.G. SBA-15-supported gold nanoparticles decorated by CeO_2: Structural characteristics and CO oxidation activity. *Appl. Catal. A Gen.* **2010**, *381*, 42–53. [CrossRef]
69. Laha, S.C.; Mukerjee, P.; Sainkar, S.R.; Kumar, R. Cerium containing MCM-41-type mesoporous materials and their acidic and redox catalytic properties. *J. Catal.* **2002**, *207*, 213–223. [CrossRef]
70. Pestryakov, A.N.; Lunin, V.V.; Kharlanov, A.N.; Kochubey, D.I.; Bogdanchikova, N.; Stakheev, A.Y. Influence of modifying additives on electronic state of supported gold. *J. Mol. Struct.* **2002**, *642*, 129–136. [CrossRef]
71. Pestryakov, A.N.; Lunin, V.V.; Kharlanov, A.N.; Bogdanchikova, N.E.; Tuzovskaya, I.V. Electronic state of gold in supported clusters. *Eur. Phys. J. D* **2003**, *24*, 307–309. [CrossRef]
72. Pestryakov, A.; Tuzovskaya, I.; Smolentseva, E.; Bogdanchikova, N.; Jentoft, F.; Knop-Gericke, A. Formation of gold nanoparticles in zeolites. *Int. J. Mod. Phys. B* **2005**, *19*, 2321–2326. [CrossRef]
73. Simakov, A.; Bogdanchikova, N.; Tuzovskaya, I.; Smoletseva, E.; Pestryakov, A.; Farias, M.; Avalos, M. Catalysts based on gold nanosized species incorporated into zeolites. In *Complex Mediums VI: Light and Complexity*; McCall, M.W., Dewar, G., Noginov, M.A., Eds.; SPIE: San Diego, CA, USA, 2005; Volume 5924, p. 101. ISBN 9780819459299.
74. Smolentseva, E.; Bogdanchikova, N.; Simakov, A.; Pestryakov, A.; Tuzovskaya, I.; Avalos, M.; Farías, M.H.; Díaz, J.A.; Gurin, V. Influence of copper modifying additive on state of gold in zeolites. *Surf. Sci.* **2006**, *600*, 4256–4259. [CrossRef]
75. Smolentseva, E.; Bogdanchikova, N.; Simakov, A.; Pestryakov, A.; Avalos, M.; Farias, M.H.; Tompos, A.; Gurin, V. Catalytic activity of gold nanoparticles incorporated into modified zeolites. *J. Nanosci. Nanotechnol.* **2007**, *7*, 1882–1886. [CrossRef]
76. Tuzovskaya, I.V.; Simakov, A.V.; Pestryakov, A.N.; Bogdanchikova, N.E.; Gurin, V.V.; Farías, M.H.; Tiznado, H.J.; Avalos, M. Co-existence of various active gold species in Au-mordenite catalyst for CO oxidation. *Catal. Commun.* **2007**, *8*, 977–980. [CrossRef]
77. Costa, V.V.; Estrada, M.; Demidova, Y.; Prosvirin, I.; Kriventsov, V.; Cotta, R.F.; Fuentes, S.; Simakov, A.; Gusevskaya, E.V. Gold nanoparticles supported on magnesium oxide as catalysts for the aerobic oxidation of alcohols under alkali-free conditions. *J. Catal.* **2012**, *292*, 148–156. [CrossRef]

78. Feldheim, D.L.; Foss, C.A. *Metal Nanoparticles: Synthesis, Characterization and Applications*; Dekker, M., Ed.; CRC Press: New York, NY, USA; Basel, Switzerland, 2002; ISBN 0-8247-0604-8.
79. Feng, R.; Li, M.; Liu, J. Synthesis of core-shell Au@Pt nanoparticles supported on Vulcan XC-72 carbon and their electrocatalytic activities for methanol oxidation. *Colloids Surf. A Physicochem. Eng. Asp.* **2012**, *406*, 6–12. [CrossRef]
80. Galindo-Hernández, F.; Wang, J.A.; Gómez, R.; Bokhimi, X.; Lartundo, L.; Mantilla, A. Structural modifications in Au/Al_2O_3–CeO_2 mixed oxides as a function of Ce^{4+} content and its effects in the mineralization of the herbicide diuron. *J. Photochem. Photobiol. A Chem.* **2012**, *243*, 23–32. [CrossRef]
81. Guzmán, C.; del Ángel, G.; Gómez, R.; Galindo-Hernández, F.; Ángeles-Chavez, C. Degradation of the herbicide 2,4-dichlorophenoxyacetic acid over Au/TiO_2–CeO_2 photocatalysts: Effect of the CeO_2 content on the photoactivity. *Catal. Today* **2011**, *166*, 146–151. [CrossRef]
82. Irie, H.; Miura, S.; Kamiya, K.; Hashimoto, K. Efficient visible light-sensitive photocatalysts: Grafting Cu(II) ions onto TiO_2 and WO_3 photocatalysts. *Chem. Phys. Lett.* **2008**, *457*, 202–205. [CrossRef]
83. Qiu, X.; Miyauchi, M.; Sunada, K.; Minoshima, M.; Liu, M.; Lu, Y.; Li, D.; Shimodaira, Y.; Hosogi, Y.; Kuroda, Y.; et al. Hybrid Cu_xO/TiO_2 Nanocomposites as Risk-Reduction Materials in Indoor Environments. *ACS Nano* **2012**, *6*, 1609–1618. [CrossRef] [PubMed]
84. Chary, K.V.R.; Sagar, G.V.; Naresh, D.; Seela, K.K.; Sridhar, B. Characterization and reactivity of copper oxide catalysts supported on TiO_2-ZrO_2. *J. Phys. Chem. B* **2005**, *109*, 9437–9444. [CrossRef] [PubMed]
85. Dong, L.; Liu, L.; Lv, Y.; Zhu, J.; Wan, H.; Liu, B.; Gao, F.; Wang, X.; Dong, L.; Chen, Y. Surface structure characteristics of $CuO/Ti_{0.5}Sn_{0.5}O_2$ and its activity for CO oxidation. *J. Mol. Catal. A Chem.* **2012**, *365*, 87–94. [CrossRef]
86. Liu, Z.; Amiridis, M.D.; Chen, Y. Characterization of CuO Supported on Tetragonal ZrO_2 Catalysts for N_2O Decomposition to N_2. *J. Phys. Chem. B* **2005**, *109*, 1251–1255. [CrossRef]
87. Sobczak, I.; Wolski, Ł. Au–Cu on Nb_2O_5 and Nb/MCF supports–Surface properties and catalytic activity in glycerol and methanol oxidation. *Catal. Today* **2015**, *254*, 72–82. [CrossRef]
88. Kaminski, P.; Sobczak, I.; Decyk, P.; Ziolek, M.; Roth, W.J.; Campo, B.; Daturi, M. Zeolite MCM-22 Modified with Au and Cu for Catalytic Total Oxidation of Methanol and Carbon Monoxide. *J. Phys. Chem. C* **2013**, *117*, 2147–2159. [CrossRef]
89. Kaminski, P.; Ziolek, M. Surface and catalytic properties of Ce-, Zr-, Au-, Cu-modified SBA-15. *J. Catal.* **2014**, *312*, 249–262. [CrossRef]